ELSEVIER

Chemical Engineering Journal 101 (2004) 113–121

Chemical Engineering Journal

www.elsevier.com/locate/cej

Wall coating of a $CuO/ZnO/Al_2O_3$ methanol steam reforming catalyst for micro-channel reformers

Jaime Bravo, Ayman Karim, Travis Conant, Gabriel P. Lopez, Abhaya Datye*

Department of Chemical and Nuclear Engineering, Ceramic and Composite Materials Center,
University of New Mexico, Albuquerque, NM 87131-1341, USA

Abstract

Capillaries of quartz and fused silica were coated with a commercial BASF $CuO/ZnO/Al_2O_3$ catalyst. The objective was to create micro channels with reactive coatings for steam reforming of methanol to produce H_2 for proton exchange membrane (PEM) fuel cells. A slurry of catalyst with a boehmite binder was filled in the capillary and then displaced by a stream of inert gas. This gas displacement method allowed us to generate coatings ranging from 1 to 25 μm in thickness by varying the slurry viscosity. The 25 μm coating thickness was deposited on a range of tube diameters, for example 4.1 mm, 2 mm, and 530 μm diameter. The coating was adherent and did not peel off during catalytic reaction tests which lasted up to 10 days. The activity of the coated catalyst was superior to that of the same catalyst in a packed bed.

Keywords: Wall coating; Methanol; Reformers; Microreactors

1. Introduction

Methanol is being considered as a primary liquid fuel for generating hydrogen for proton exchange membrane (PEM) fuel cells to be used in small portable devices. The low temperatures required for steam-reforming of methanol make it possible (with elevated temperature PEM fuel cells) to utilize reformate without subsequent processing to remove CO, which is a poison for the PEM anode electrocatalyst [1]. The group of catalysts that shows the highest activity at low temperature has composition of $CuO/ZnO/Al_2O_3$, which is also the catalyst used for methanol synthesis [2]. Steam reforming of methanol is a highly endothermic process. Conventional reactor configurations, such as a packed bed reactor, operate in a heat transfer limited mode for this reaction. Using the catalyst in packed bed form for portable devices is also not convenient due to high pressure drop and possible channeling of gases in addition to poor heat transfer. A wall-coated catalyst represents a superior geometry since it provides lower pressure drop, ease of manufacturing and eliminates pressure drop due to form drag.

Due to their small size, microreactors are especially suited for endothermic reactions whose reactivity depends on the rate of heat input. The isothermal behavior of microreactors is specifically due to their ability to efficiently transfer heat. That is one of their great strengths as a tool for process intensification, where the catalyst, products, or process may be sensitive to temperature. The isothermal operation of microreactors and micro-heat-exchangers has been reported by numerous researchers. The earliest demonstration of the isothermal operability of a micro-heat-exchanger was in the computer industry. A silicon micro-heat-exchanger built by conventional VLSI manufacturing techniques was shown by Tuckerman and Pease [3] to achieve high heat transfer rates for cooling a central processing unit in a computer.

Researchers at BASF also used the heat transfer benefits of microreactors for scale-up of a oxidative dehydrogenation reaction: $RCH_2OH + (1/2)O_2 \rightarrow RCHO + H_2O$. This reaction is exothermic and operates at about 500 °C over an elemental silver catalyst. Production was carried out in 5 cm diameter pan-like reactors where a 2 cm thick layer of powder catalyst was placed over a gas-permeable plate, with a selectivity of 90% being achieved at a conversion of 50%. A solid silver micro-heat-exchanger was built to operate isothermally and the selectivity and conversion were improved to 96 and 55%, respectively [4].

Due to their origins from the semiconductor industry, most microreactor fabrication techniques involve silicon wafer processing methods such as wet/dry etch, lithography, thin film deposition and integration procedures. These techniques have also been extended to glass wafers to create complex three-dimensional designs. Steel alloys and aluminum plates have been widely employed for manufacture of microreac-

---

* Corresponding author. Tel.: +1-505-277-0477; fax: +1-505-277-1024.
E-mail address: datye@unm.edu (A. Datye).

1385-8947/$ – see front matter © 2004 Elsevier B.V. All rights reserved.
doi:10.1016/j.cej.2004.01.011

tors. Plates are micromachined or patterned with lithography techniques and attached by diffusion bonding to form monolithic structures. Extruded alumina parts have also been used in the assembly of microreactors [5]. The least cited method is fabrication by tape-casting. Tape-casting involves the layering of unsintered alumina-based green tape. Prior to layering, the sheets are patterned and etched in one step by a laser. The patterned layers can be stacked >80 layers high and co-fired at elevated pressures and temperatures to form three-dimensional structures. Tape-casting can create features down to 10 μm [6].

All of the microreactor types described here require a solid catalyst to catalyze the gas phase reactions being carried out. To eliminate the problems of catalyst coating and deposition, BASF researchers simply built their micro-heat-exchanger reactor out of solid silver which was the catalyst for their reaction. Combustion of hydrocarbons is done over a palladium metal catalyst. Manufacturing a solid palladium microreactor is not feasible from an economic perspective. Current methods for loading microreactors with catalysts include packing the catalyst in a bed [7–10]. Packed bed reactors are not the most efficient design as size is scaled down, due to large pressure drop, as predicted by the Ergun equation [11]. Also, channeling at the wall-particle interface becomes increasingly likely for creeping flow in microreactors. If the packed bed catalyst sinters, there will be an increased pressure drop due to the reduction in the void fraction. One benefit of packed bed reactors is that commercial catalysts formulations that have already been optimized may be used. In contrast VLSI manufacturing methods (PVD, CVD) provide alternative approaches for deposition of thin catalyst films, however these thin film deposition techniques may not provide the high surface area required for catalytic reactions and are restricted to elemental catalysts. Other methods to generate high surface areas in thin films include anodic oxidation of silicon [12] or aluminum [13–15] surfaces through electrolysis or thermal oxidation of aluminum rich steel [16]. These methods of creating porous structure are limited to sub micron layers. None of these methods are suitable for the methanol steam reforming reaction.

Deposition of thin porous silica films through sol gel processing [17–19] has been done on flat or corrugated [20] substrates with the use of dip and spin coating methods. A major limitation is that dip and spin coating processes are limited to deposition of wash coats on carrier plates followed by reactor assembly. Although, this method is acceptable for laboratory studies it proves to be too costly for a commercial devices used for portable power generation. Processes such as wall coating channels of millimeter dimension for monoliths used as catalytic converter in automobiles have been done for decades. However, the adhesion of the wash coat is known to be a function of substrate porosity [21,22]. Methods of creating porosity on silicon, aluminum, and stainless steel surfaces have been used to prepare surfaces for wash coating of micro channels. However, these methods are manufacturing intensive. A new challenge is to wall coat non-porous microchannels with alumina wash coats in a controlled and economic fashion, post reactor assembly.

In this paper, we report our initial study of coating methods for pre-assembled microreactor configurations. The specific problem we have addressed is the application of a thick catalyst coat to a non-porous surface such as quartz, fused silica or ceramic tape. We have utilized a fully formulated commercial catalyst such as BASF F13456 $CuO/ZnO/Al_2O_3$. The catalyst wall coats were applied to a tubular reactor where the reactor diameter was varied from 4.1 mm all the way down to 250 μm. Catalyst adhesion to the glass surface was a significant challenge. Our work shows that the development of methods to coat catalyst powders without affecting their activity remains a key challenge in developing microreactors for mobile applications.

2. Experimental

Our approach was to select a geometry that was easy to characterize for repeated experiments. Quartz capillaries with inner diameters of 4.1 and 2 mm were used, as well as fused silica capillaries used in gas chromatography with inner diameters of 530 and 250 μm. The capillaries were coated using the gas displacement method. Boehmite was used as a binder. Controlled gelation of the boehmite gels allowed us to vary the viscosity of the slurry and to investigate the effect of viscosity on the coating thickness. The capillaries were characterized for wall coat thickness with a SEM and their activity for steam reforming of methanol was also investigated.

2.1. Slurry preparation

The gels were prepared by adding boehmite (Catapal from Sasol Chemie GmbH), deionized (DI) water, and nitric or hydrochloric acid, to a 300 ml ball mill jar with 6 mm zirconia griding media. The boehmite powder was dispersed (deflocculated) with either nitric or hydrochloric acid prior to the gelation step: with proportion 10–20 wt.% Boehmite, 1 wt.% conc. HCl and balance DI water. Further acid was added in the subsequent gelation step, 0.75 to 3 ml 1N HCl. The amount of acid added was determined by the desired viscosity and gelation time. For the catalytic slurries, a commercially available BASF F13456 $CuO/ZnO/Al_2O_3$ catalyst was used in this study. The catalyst is available in the form of 3 mm extruded pellets. The pellets were ground by hand into coarse powder in a mortar and pestle. The catalyst was then added to the ball mill jar in the dispersing step. The dispersing step was done overnight. Initially the $CuO/ZnO/Al_2O_3$ catalyst and boehmite were loaded into the milling jar with DI H_2O in the mass ratios of 44:11:100. The ratio was varied to change the viscosity of the slurry. Boehmite serves as the binder and dispersant for the catalyst particles in the film. Boehmite has been proven successful as a binder in extruded ceramic processing [19,23–25]. The viscosities of the slurries were measured with a plate and cone viscometer.

2.2. Coating procedure

The coating procedure consists of first washing the surface with hot sulfuric acid/solid-oxidizer mixture for 30 min at 100–120 °C. The solid oxidizer used in this paper is NOCHROMIX® from GODAX Laboratories, Inc., Cat Number 19-010. The sulfuric acid/solid mixture is called piranha etch in this paper. The surfaces were rinsed with DI H_2O followed by ethanol and dried in an oven at 80 °C. This step was performed to remove organic material from the surface as well as to increase the extent of hydroxylation of the glass surface. The coating process was performed by gas assisted fluid displacement, a method used for coating walls of capillaries. The process is done in two steps: (1) filling the capillary with a viscous fluid, and (2) clearing the capillary by forcing gas through it. Fig. 1 shows a diagram of the process. When air is forced into one end of a capillary, containing a viscous fluid, a bubble forms at the front end. The bubble travels down the capillary forcing some of the liquid, leaving behind a fraction in the form of a film covering the wall of the capillary.

2.3. Catalytic activity tests

The reactor consists of a 4.1 mm quartz tube positioned in an aluminum block heated by two cartridge-heaters. The temperature of the aluminum block was controlled by a temperature controller. The inlet and outlet temperatures of the reactor were also monitored. The reactor effluent stream passed through a gas-sampling valve, then through a condenser to trap unreacted water and methanol before reaching a digital mass flow meter which allowed for total product gas flow to be monitored. The effluent of the reactor was analyzed using a Varian CP-3800 gas chromatograph (GC) equipped with a Porapak Q column and a TCD detector, using helium as the carrier gas. The analysis of the gas phase species CO_2, CO and CH_3OH along with a carbon balance allowed the methanol conversion and CO selectivity to be calculated. The GC was programmed to sample reactor product gases at 30 min intervals around the clock. The entire system was automated by Labview software and appropriate data acquisition hardware.

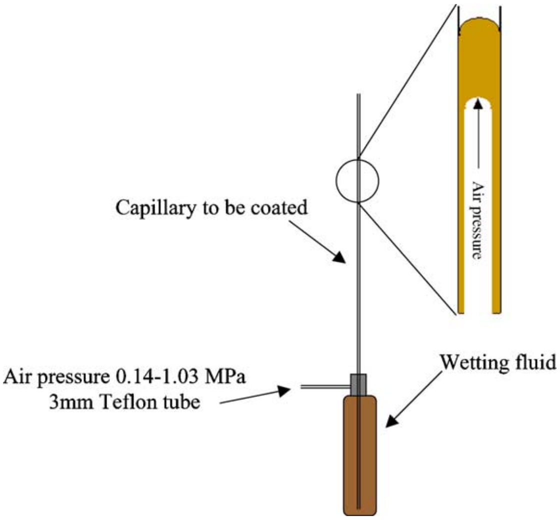

Fig. 1. Experimental setup for wall coating of capillaries. Air pressure forces the wetting fluid through the capillary leaving behind a thin film. The magnified view of the capillary shows a schematic of the coating achieved by gas-assisted displacement of a slurry.

The $CuO/ZnO/Al_2O_3$ catalyst was used in its received, calcined state. The reactor was heated to the reaction temperature of 230 °C under helium flow of 4 sccm at 15 °C/min. The helium was left to flow for an hour after the temperature reached 230 °C before the water methanol mixture was introduced to the reactor. A mixture of 1:1.1 molar methanol/water was pumped using an injection pump (Cole Parmer 74900) at 0.2 ml/h to a custom in-house built vaporizer operating at 130 °C. The vaporizer was optimized to get a stable flow rate and minimize fluctuations in the water–methanol molar ratio. The kinetic data were collected during the first 3 h of starting the methanol/water flow, no catalyst deactivation was observed. In some cases reaction tests were carried out for 10 days to test for catalyst coat adhesion. The data collection procedure was the same for both the wall coated and packed-bed reactor configurations.

2.4. Film thickness measurements

Scanning electron microscopy was used to measure the thickness of the catalyst coat in the capillaries. A Hitachi S-800 microscope was used for these measurements. The quartz capillaries were scribed and cleaved to obtain cross-section samples.

The liquid film thickness after gas displacement was also measured for the pure boehmite gel samples as described next. A micro molar amount of fluorescein was mixed into the boehmite gel sample for coating. A laser with wavelength of 488 nm was used to excite fluorescein in the gel. A filter was used to cut off all wavelengths below 500 nm prior to detection. The fluorescence of the completely filled capillaries was compared to the fluorescence of the wall coated capillary at a wavelength of 515 nm. From the ratio of intensity, the amount of liquid remaining in the capillary could be derived. Knowing the capillary dimension, the intensity measurement could be used to derive liquid film thickness.

3. Results

The seminal work on the coating of capillaries with thin liquid films was done by Taylor [26]. In his work, he showed that a thin film of liquid would be left behind when a filled capillary was purged with a stream of gas. Fig. 1 shows a schematic diagram of our experimental setup for coating of capillary tubes, which is similar to that used by Taylor. Taylor's work correlated the film thickness of the coating fluid as a function of the capillary number, $Ca = \mu u/\sigma$, for a circular capillary. In this equation, μ is the fluid viscosity, u is the displacing gas velocity and σ is the surface tension of the coating liquid. The maximum wall coat achieved was 56% of the capillary cross-section as the *Ca* number approached a value of 2 in Taylor's work. Other researchers have obtained 67% with the aid of improved apparatus [27]. The diameters of capillaries coated in Taylor's experiments ranged from 1.5 to 4 mm.

In our experiments, the primary variable was the viscosity of the coating fluid. We prepared catalyst wash coat slurries and pure boehmite gels, each with different solid loadings and acid content. This was done to achieve different viscosities. In this way the catalytic wash coat slurry viscosity was varied between 150 and 250 cP, as shown in Fig. 2. The non-Newtonian behavior of the boehmite gel solutions was very similar to that of Fig. 2. It was easier to tune the viscosities of the boehmite gels due to the interaction among the boehmite crystallites. Thus, to understand the coating behavior we started with gel samples.

The coating experiments were performed with boehmite gel solutions (without catalyst) using 250 and 530 μm capillaries. The extent of gelation of boehmite slurries was more easily controlled. The boehmite gels were used to find the limit of the capillary coat thickness for a given capillary diameter. The viscosities were varied in the range of 100–1000 cP by simply changing the boehmite and acid content. The thickness of the gel coats was measured with fluorescence intensity measurements. The capillaries were stripped of their exterior polymeric coating with a hot piranha etch. The coat thickness was derived through a linear interpolation of the fully filled capillary fluorescence intensity to that of the coated capillary, see Figs. 3 and 4. However, we encountered a problem with the 250 μm capillaries, since they formed discrete plugs as opposed to a uniform wall coat, as shown in Fig. 5. Fig. 6 shows a schematic diagram of the coating process which may lead to formation of the plugs shown in Fig. 5.

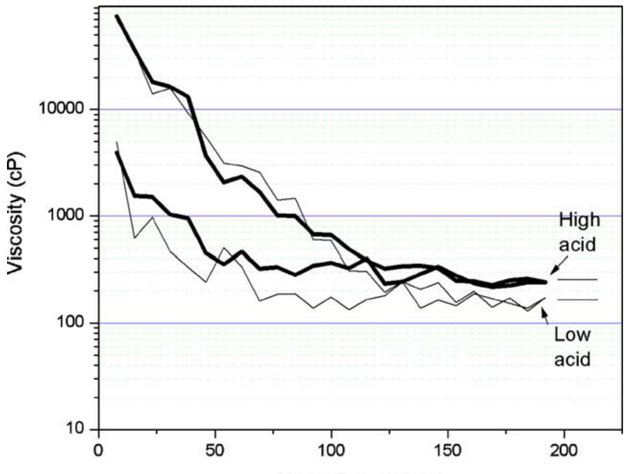

Fig. 2. The viscosity of the catalyst slurries as function of shear rate. The slurry consisted of 7 wt.% boehmite, 28 wt.% catalyst, 1 wt.% of HCl in concentrated form with the balance being DI water. Four milliliters of 1N HCl was added to drive the condensation reaction (the light line) and an additional 5.25 ml of 1N HCl was added (the heavy line). It is seen that the viscosity at high shear rates increased from 150 to 250 cP with increased acid addition. Each of the two curves shows the hysteresis between the viscosity at decreasing and increasing shear rates.

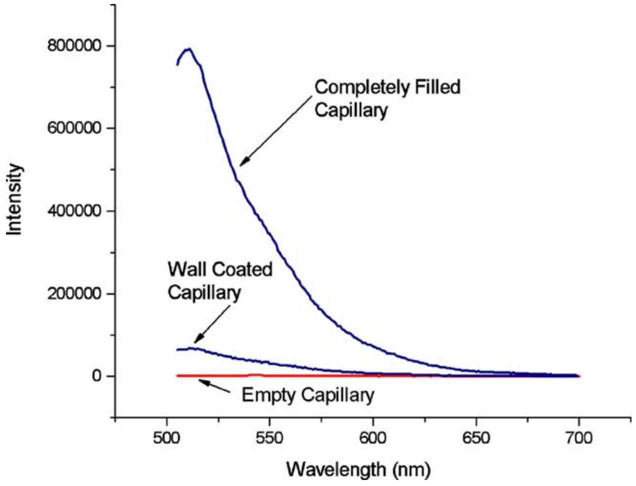

Fig. 3. Fluorescence intensity measurements of a 530 μm wall coated and completely filled capillary. The incident laser had a wavelength of 488 nm. A filter was used to remove all emissions below 500 nm. The exterior polymer coating on the fused capillary capillaries was removed to facilitate fluorescence intensity measurements at selected locations.

Initially, the coating experiments for the catalytic slurry of $CuO/ZnO/Al_2O_3$ were done without the addition of acid. A minimal coat of less than one micron was observed. Coverage was not uniform and only random patches were observed. The necessity of the acid is two-fold: it activates the boehmite to go through condensation reactions with

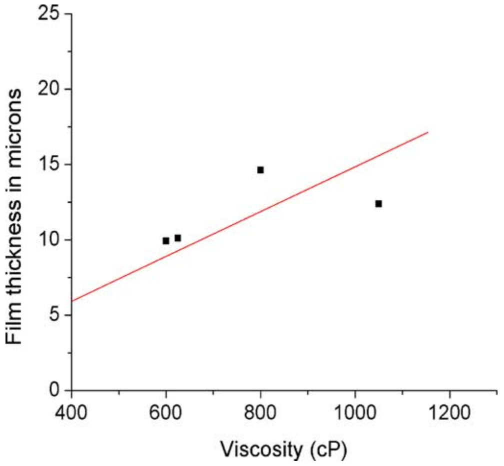

Fig. 4. A plot of liquid film thickness (from measurements such as those in Fig. 3) as a function of viscosity. All capillaries were 530 μm in diameter and the only parameter varied was viscosity.

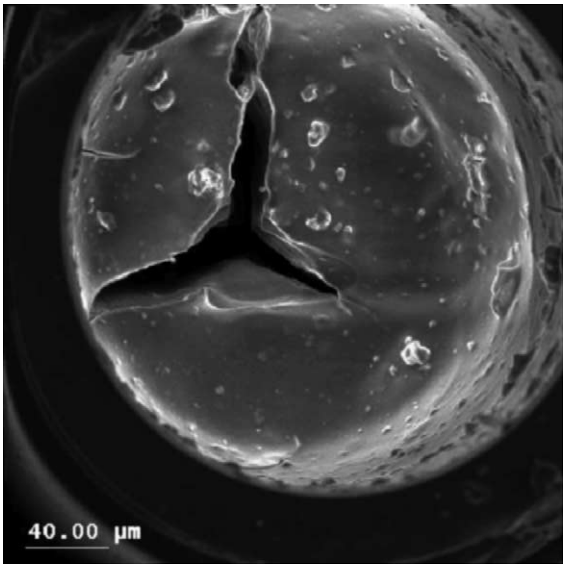

Fig. 5. SEM image of a cross section of a failed attempt to coat a 250 μm capillary with an alumina gel. The alumina formed a discrete plug that blocked the flow through the capillary.

other boehmite particles, as well as bonding them to the hydroxylated surface of the microchannels. Fig. 7 shows a $CuO/ZnO/Al_2O_3$ coat in a 530 μm capillary. The slurry consisted of 7 wt.% boehmite, 28 wt.% catalyst, 1 wt.% of HCl in concentrated form, balance DI water, for dispersion. An additional 4 ml of 1N HCl was added to drive the condensation reaction for 6 h. The viscosity of the slurry was about 150 cP. The parallel grooves seen in the image show the effect of large particles ($CuO/ZnO/Al_2O_3$) in the slurry. Fig. 8 was a controlled experiment where the viscosity was increased through the addition of boehmite, where a thicker coating could be generated. These figures demonstrate the ability of this process to coat the inside of capillaries with a catalytic film of $CuO/ZnO/Al_2O_3$.

The activity of the wall coated catalysts was tested with 4.1 mm i.d. quartz tubes that were wall coated or alternatively were packed with 75 and 100 mg of catalyst. Fig. 9 shows the methanol conversion versus space time W/F_{CH_3OH} (kg catalyst)/(mol/s of methanol) for both reactors. A kinetic model first order in methanol was fit to the data and is shown in solid lines. Fig. 10 shows the CO selectivity versus methanol conversion. The CO selectivity was calculated from the partial pressures, $[P_{CO}/(P_{CO_2} + P_{CO})] \times 100$. Both reactor configurations showed low catalyst selectivity towards CO, which is very desirable. The wall coated catalyst had a lower CO selectivity than the packed bed configuration, as shown in Fig. 10. The highest mole %CO in the effluent stream from the wall coated reactor was 0.57% at a methanol conversion of 96.5%.

4. Discussion

Extensive research has been done on wash coating methods for catalyst deposition in honeycomb monoliths used as catalytic converters for automobiles. The procedure is similar to that outlined in this paper. Typically, the monoliths are acid washed, rinsed and dried to clean the porous surface of the monoliths. Then, a slurry wash-coat is applied to deposit catalyst on the surface. The wash coats are then sintered to yield an adherent catalyst coating. The adhesion strength of the wash coat to the monolith surface is a function of porosity of the surface, and also the temperature history of calcination. The porosity of the ceramic monolith surface is typically 30–50% with mean pore size in the range of 3–20 μm. The larger pore sizes yield higher adhesion strengths [22,28]. Similar wash coat techniques have been used for the manufacturing of wall coated microreactors. Researchers have used thermal oxidation of aluminum rich steel to create a porous Al_2O_3 layer to enhance the wash coat adhesion on microchannels [16,29]. Anodic oxidation of alumina [13] and silicon [12] has also been used to create porosity on the surface of microchannels. In these systems, the adhesion of the wash coat is determined by the ability of the wash coat to branch into the pore space through capillary forces and adhere mechanically after the films have been calcined.

Since our work is devoted to coating of non-porous surfaces, a critical factor is achieving enough adhesion to the reactor wall. To test the adhesion, our initial measurements

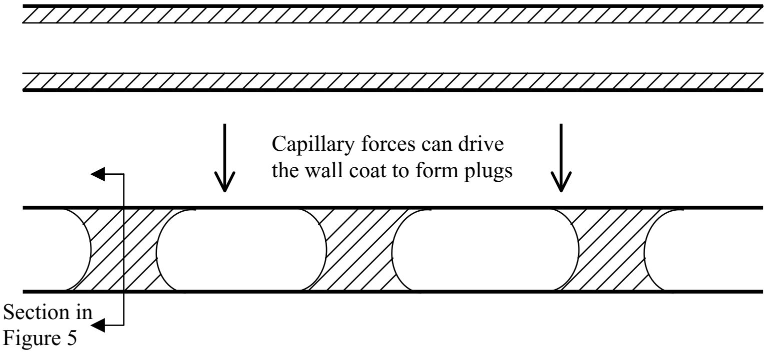

Fig. 6. Cross-section view of a circular capillary after gas displacement, leading to a uniform thin film coating (top). The schematic below shows how the capillary pressure could cause the wall coat to collapse into discrete plugs. An SEM image of the cross section of such a plug is shown in Fig. 5.

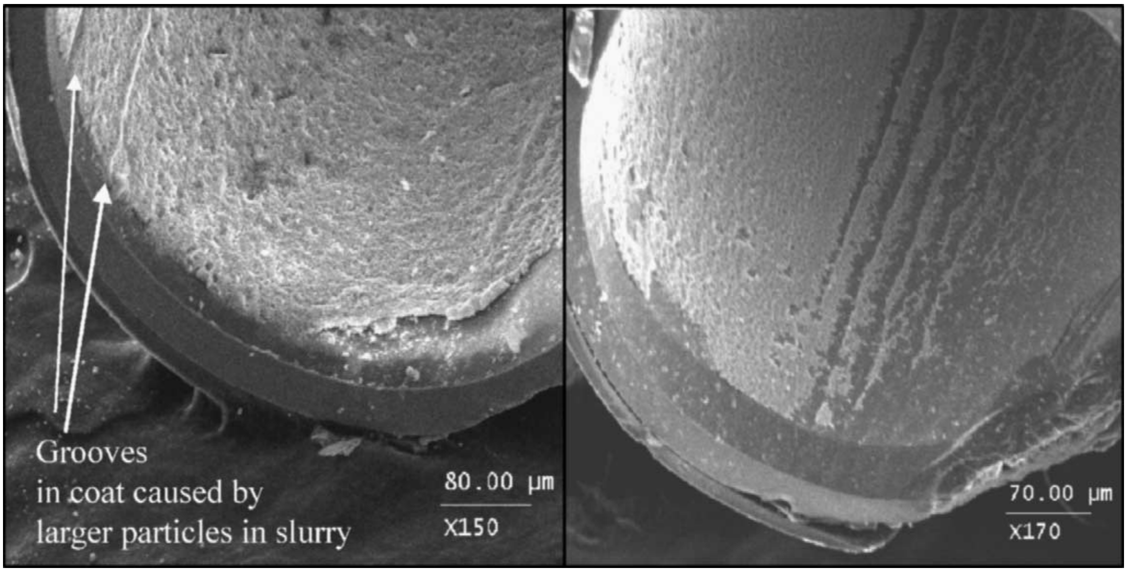

Fig. 7. $CuO/ZnO/Al_2O_3$ catalyst coating on 530 μm fused silica capillaries. Nitric acid was used to gel the slurry. The film thickness varied from 0 to 10 μm. The gas pressure used was 0.28 MPa for a 30 cm segment. Both SEM images are of the same sample at different locations.

were made with flat pieces of glass, fired ceramic green tape and silicon wafers. A jet of high pressure air (0.4 MPa) through a 6 mm i.d. tube was directed perpendicular to the surface. The coatings were evaluated in a pass or fail mode, fail if the coatings peeled or flaked off. The films were deposited by dip coating. Glass and silicon coupons achieved adequate adhesion after the surface was cleaned by sonication with ethanol. However, the ceramic green tape could not be dip coated after the same ethanol pretreatment. Contact angle measurements of water on the green tape surface showed a value of 57°. The thermodynamic reversible work of adhesion W_r can be correlated to the contact angle θ through the Dupré–Young equation [30]:

$$W_r = \sigma_{lg}(1 + \cos\theta) \tag{1}$$

where σ_{lg} is the surface tension of the coating fluid in air. From Eq. (1), it is evident that the work of adhesion is maximized when the contact angle θ is zero or we have near complete wetting of the fluid. XPS results of the sonicated coupon revealed a significant amount of carbon on the surface. We found that a hot piranha etch was able to clean the ceramic surfaces. The etched green tape coupons now

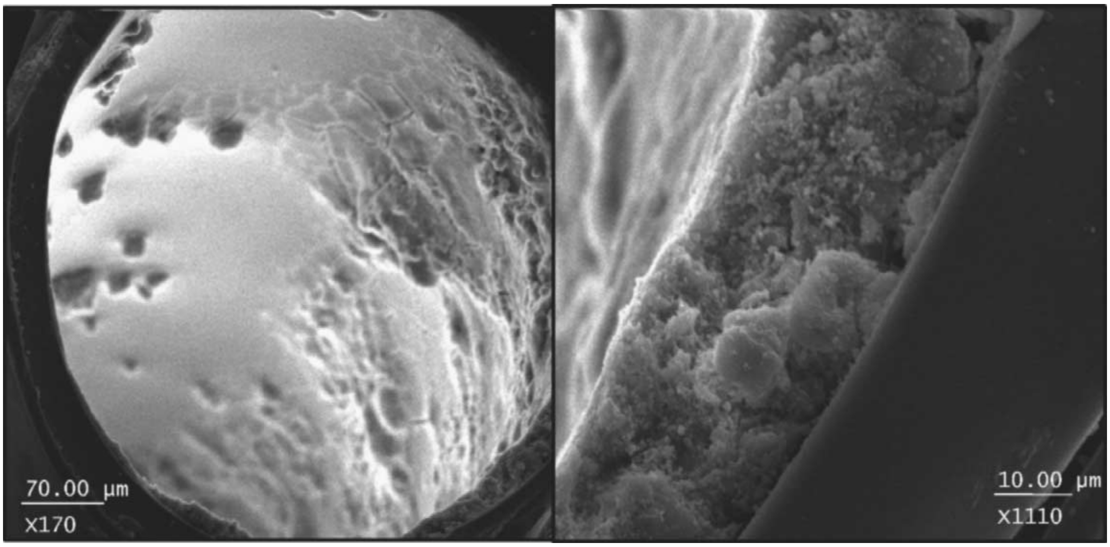

Fig. 8. $CuO/ZnO/Al_2O_3$ catalyst coating on 530 μm fused silica capillaries. The film thickness varied from 3 to 25 μm. The gas pressure used was 0.4 MPa for a 30 cm segment and the viscosity of this sample was increased over that in Fig. 7. The image on the right is a higher magnification view of the sample on the left.

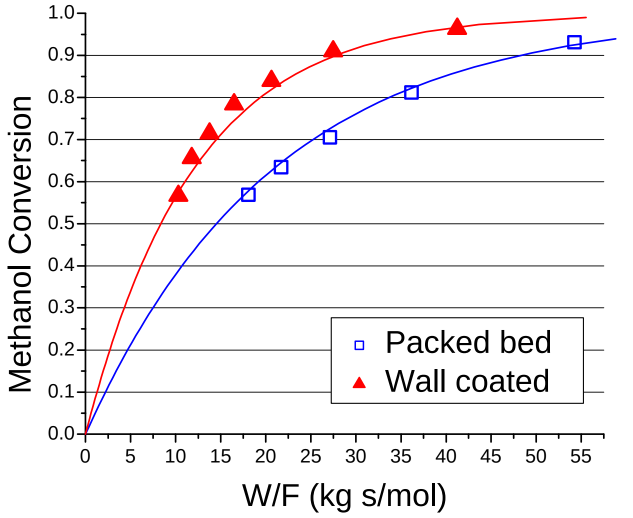

Fig. 9. Reactivity for methanol steam reforming reaction for a packed bed and wall coated reactors with $P = 640$ Torr and $T = 230\,^{\circ}\mathrm{C}$. The packed bed reactor consists of a 4.1 mm i.d. quartz tube, the reaction zone is 8.5 mm long packed with 100 mg (100–250 μm) particles. The wall coated reactor was coated using the method described in this paper, the weight of the catalyst was 75 mg on a length of 18 cm of the quartz tube. Solid lines correspond to a first order kinetic model with respect to methanol.

showed a complete wetting behavior, where a small drop of DI water completely covered the coupons. After this pretreatment, it was possible to coat the green tape surface and achieve adherent coatings. To minimize stresses during drying, slow heating ramp rates of 1 °C/min were used.

When this method (sonication in ethanol followed gas-assisted displacement) was applied to 4 mm i.d. capillaries, suitable catalyst coatings could be deposited. However, with the 2 mm quartz and 530 μm fused silica capillaries, the slurries were completely washed out when air pressure was applied. In an effort to increase the work of adhesion, the capillaries were also treated with a piranha etch while using the same coating system shown in Fig. 1. After the etch treatment of the 2 mm capillary, a 15 μm thick film of $CuO/ZnO/Al_2O_3$ catalyst was deposited. The piranha etch proved to be an essential part of the coating procedure and only the etched capillaries were able to be coated with adherent coatings of catalyst.

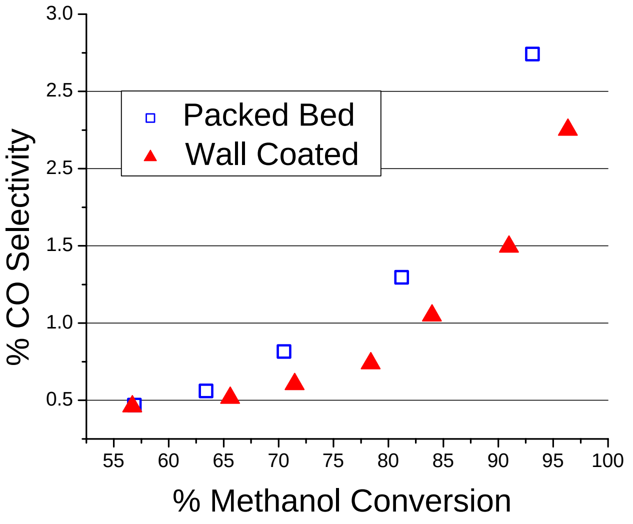

Fig. 10. CO selectivity ($CO/CO + CO_2$)versus methanol conversion for packed bed and wall coated reactors. The reaction conditions are the same as those in Fig. 9.

The next step was to be able to control the thickness of the deposited catalyst film. According to work of Taylor [26], the deposited film thickness should increase with an increase in viscosity. Fig. 2 shows how the viscosity of a catalyst slurry solution could be changed from 150 to 250 cP with the addition of nitric acid. The acid serves to catalyze the condensation reaction between surface hydroxyls. Although, the viscosity of the solution in Fig. 2 may have increased on its own without adding more acid, the time scales of gelation would be on the order of weeks to months. To achieve gelation on the time scale of minutes to hours, increasing amounts of acid were required. When boehmite gel slurries (without $CuO/ZnO/Al_2O_3$ catalyst) were prepared using HCl as the condensation catalyst, we were able to obtain viscosities in the range of 100–1000 cP.

We wanted to study the effect of slurry viscosity on the thickness of liquid films deposited using the setup in Fig. 1. Weighing the tube was not sensitive enough to determine the amount of liquid film deposited. Hence, the approach we selected was to measure fluorescence emission intensity and correlate it with the liquid film thickness. Fig. 3 shows the data collected from a 530 μm capillary coated with a boehmite gel. The fluorescence approach is non-destructive and may be extended to in situ coating experiments of thin films in glass capillaries. This technique can be used to measure the liquid films deposited in extremely small capillaries. The amounts of fluorescein added are in the micromolar range and are not expected to affect the properties of the gel significantly. Fig. 4 is a plot that shows our initial experiments on liquid film thickness as a function of viscosity, with all other factors maintained constant. The limited data available so far shows increasing liquid film deposited on the capillary walls as the fluid viscosity was increased, which is consistent with Taylor's correlation [26]. It is expected that the coat thickness should vary between zero and a maximum value.

Identical experiments done on 250 μm capillaries showed a tendency to form discrete plugs in the entire viscosity range of 100–1000 cP, although, the number and size of plugs varied with viscosity. This suggests that the size of the capillary may be an important factor. Unlike previous work which has always assumed that the fraction of liquid film left behind was dependent only on the capillary number. There was no explicit lower limit to the size of the capillary or channel being coated. However, it is apparent that in microchannels, the curvature of the microchannel could play an important role in determining the coating behavior. For the coat to be stable, the fluid needs to withstand the capillary pressure given by the Young-Laplace equation:

$$\Delta P = \sigma \left(\frac{1}{r_1} + \frac{1}{r_2} \right) \qquad (2)$$

were ΔP is the capillary pressure and r_1 and r_2 are the two radii that determine curvature. Here, r_1 is infinity and r_2 is the radius of inner diameter after coating. The capillary pressure will clearly increase with a lowering of channel diameter. At some point, a fluid instability may lead the fluid to fill the entire cross-section, rather than form a thin film as shown in the schematic diagram in Fig. 6. By modifying the coating fluid properties, such as surface tension and viscosity, we may be able to achieve thicker coatings in narrow capillaries. Future work will be directed at understanding these effects in micro capillaries.

Figs. 7 and 8 show SEM images of catalyst coatings in the 530 μm fused silica. With the increase of viscosity the coat thickness doubled. The adhesion strengths of the coat is excellent since they can withstand air pressure difference of 0.4 MPa over a 30 cm length. An important objective of this study was to investigate the effect of the slurry coating on catalyst activity. Fig. 9 shows a comparison of the activity of the wall coated catalyst with a packed bed. Detailed analysis of the heat and mass transfer limitations shows that the 4.1 mm inner diameter reactor in packed bed configuration is subject to heat transfer limitation during the steam reforming of methanol [31]. However, the packed bed is free of internal and external mass transfer limitations according to the Weisz-Prater and Mears criteria [11], respectively. The packed bed suffers from large temperature gradients and the measured activity is lower than the intrinsic activity of the catalyst. To eliminate temperature gradients in a packed bed reactor of this size, high space velocities, diluent gas and catalyst dilution would be necessary. For a commercial reformer, where volume needs to be minimized and pure water and methanol will be used, reactor inner diameter of 300–450 μm would be necessary to eliminate temperature gradients [32]. On the other hand, the wall coated reactor was found to be free from any transport limitations and this can be seen in its higher measured catalyst activity [31]. Detailed discussion and experimental study of the wall coated and packed bed reactors will be presented elsewhere [32]. Since the packed bed is heat transfer limited, the reactivity comparison presented here is not strictly accurate. However, one conclusion from the data presented here is that the catalyst activity has not deteriorated with the processing involved in transforming 3 mm extruded pellets of a commercial BASF $CuO/ZnO/Al_2O_3$ catalyst onto finely divided catalyst that was deposited on smooth microchannel surfaces.

5. Conclusions

The work has been directed at developing catalyst coatings in microchannels for the methanol steam reforming reaction. We have taken 3 mm extruded pellets of a fully formulated, commercial BASF $CuO/ZnO/Al_2O_3$ catalyst and developed coatings of 25 μm thickness in channels as small as 530 μm in diameter. The catalytic activity of the wall coated catalyst was compared to a packed catalyst bed using a 4.1 mm i.d. tube. We found that the apparent catalyst activity of the wall coated catalyst showed improvement over the same catalyst in packed bed form. Methods to control the thickness of a liquid film coating using controlled gelation of boehmite slurry were developed. It was found that in the 250 μm channel, the deposited thin films became metastable and capillary forces caused the film to form discrete plugs that blocked fluid flow in the capillary. The work shows the feasibility of wall coating 25 μm thick coats of $Cu/ZnO/Al_2O_3$ catalyst on non-porous surfaces such as quartz, fused silica. With this approach, we can us pre-assembled microreactors and achieve wall coatings in a cost effective manner.

Acknowledgements

The authors would also like to thank Menake E. Piyasena for assistance with fluorescence measurements. Financial support for this work was provided by the Power and Energy Consortium sponsored by the US Army Research Laboratory under the Collaborative Technology Alliance Program, Cooperative Agreement DAAD19-01-2-0010. We thank BASF for supplying $CuO/ZnO/Al_2O_3$ catalyst and SASOL for the providing us with boehmite alumina samples.

References

[1] B.A. Peppley, J.C. Amphett, L.M. Kearns, R.F. Mann, Methanol-steam reforming on Cu/ZnO/Al2O3 catalysts. Part 2. A comprehensive kinetic model, Appl. Catal. A: Gen. 5 (179) (1999) 31–50.
[2] L.F. Brown, A comparative study of fuels for on-board hydrogen production for fuel-cell-powered automobiles, Int. J. Hydrogen Energy 26 (2001) 381–397.
[3] D.B. Tuckerman, R.F.W. Pease, High-performance heat sinking for VLSI, IEEE Electron Device Lett. 126 (1981) EDL-2.
[4] O. Wörz, K.P. Jäckel, T. Richter, A. Wolf, Microreactors—a new efficient tool for reactor development, Chem. Eng. Technol. 24 (2001) 138.
[5] R. Knitter, D. Gohring, P. Risthaus, Hausselt, Microfabrication of ceramic microreactors, Microsyst. Technol. 7 (2001) 85–90.
[6] X. Wang, J. Shu, H. Bau, R.J. Gorte, Fabrication of micro-reactors using tape-casting methods, Catal. Lett. 77 (2001) 173–177.
[7] K. Kusakabe, K. Tokunaga, G.B. Zhao, S. Morooka, Fabrication of parallel microchannel reactors for use in catalyst testing, J. Chem. Eng. Jpn. 35 (2002) 914–917.
[8] S.K. Ajmera, M.W. Losey, K.F. Jensen, M.A. Schmidt, Microfabricated packed-bed reactor for phosgene synthesis, AIChE J. 47 (2001) 1639–1647.
[9] S.K. Ajmera, C. Delattre, M.A. Schmidt, K.F. Jensen, Microfabricated differential reactor for heterogeneous gas phase catalyst testing, J. Catal. 25 (209) (2002) 401–412.
[10] S. K, C. Delattre, M.A. Schmidt, K.F. Jensen, Microfabricated cross-flow chemical reactor for catalyst testing, Sens. Actuators B: Chem. 28 (82) (2002) 2–3.

[11] H.S. Fogler, Elements of Chemical Reaction Engineering, second ed., Prentice-Hall, Int. Ser. Phys. Chem. Eng. Sci. (1992) 128.

[12] M.W. Losey, R.J. Jackman, S.L. Firebaugh, M.A. Schmidt, K.F. Jensen, Design and fabrication of microfluidic devices for multiphase mixing and reaction, J. Microelectromech. Syst. 11 (2002) 709–717.

[13] G. Wiessmeier, D. Honicke, Microfabricated components for heterogeneously catalysed reactions, J. Micromech. Microeng. 6 (1996) 285–289.

[14] E. Rebrov, M. de Croon, J.C. Schouten, Design of a microstructured reactor with integrated heat-exchanger for optimum performance of a highly exothermic reaction, Catal. Today 15 (69) (2001) 1–4.

[15] R. Wunsch, M. Fichtner, O. Gorke, K. Haas-Santo, K. Schubert, Process of applying Al_2O_3 coatings in microchannels of completely manufactured microstructured reactors, Chem. Eng. Technol. 25 (2002) 700–703.

[16] K. Haas-Santo, M. Fichtner, K. Schubert, Preparation of microstructure compatible porous supports by sol–gel synthesis for catalyst coatings, Appl. Catal. A: Gen. 220 (1–2) (2001) 79–92.

[17] B.E. Yoldas, Alumina sol preparation from alkoxides, Ceram. Bull. 54 (3) (1975) 289–290.

[18] C.J. Brinker, G.W. Scherer, Sol–Gel Science: The Physics and Chemistry of Sol–Gel Processing, Academic Press, New York, 1990.

[19] M.F.M. Zwinkels, S.G. Jaras, P.G. Menon, K.I. Asen, Preparation of anchored ceramic coatings on metal substrates: a modified sol–gel technique using colloidal silica sol, J. Mater. Sci. 1 (31) (1996) 6345–6349.

[20] S. Zhao, R.S. Besser, Selective deposition of supported platinum catalyst hydrogenation in a microchachined reactor, in: Proceedings of the 6th IMRET, New Orleans, LA, AIChE, 2002.

[21] A. Cybulski, J. Moulijn, Monoliths in heterogeneous catalysis, Catal. Rev.-Sci. Eng. 36 (2) (1994) 179–270.

[22] R.J. Farrauto, C.H. Bartholomew, Fundamentals of Industrial Catalytic Process, first ed., Blackie, London, 1997.

[23] A.F. Popa, S. Rossignol, C. Kappenstein, Ordered structure and preferred orientation of boehmite films prepared by the sol–gel method, J. Non-Cryst. Solids 306 (2002) 169–174.

[24] S. Ananthakumar, V. Raja, K.G.K. Warrier, Effect of nanoparticulate boehmite sol as a dispersant for slurry compaction of alumina ceramics, Mater. Lett. 43 (2000) 174–179.

[25] S. Kwon, G.L. Messing, Constrained densification in boehmite alumina mixtures for the fabrication of porous alumina ceramics, J. Mater. Sci. 15 (33) (1998) 913–921.

[26] G.I. Taylor, Deposition of a viscous fluid on the walls of tube, Fluid Mech. 10 (161) (1961).

[27] F. Kamisli, M.E. Ryan, Gas-assisted non-Newtonian fluid displacement in circular tubes and noncircular channels, Chem. Eng. Sci. 56 (2001) 4913–4928.

[28] A. Cybulski, J.A. Moulijn, Monoliths in heterogeneous catalysis, Catal. Rev.-Sci. Eng. 36 (1994) 179–270.

[29] K. Haas-Santo, O. Gorke, P. Pfeifer, K. Schubert, Catalyst coatings for microstructure reactors, Chimia 56 (2002) 605–610.

[30] R. Defay, I. Prigogine, Surface Tension and Adsorption, Longmans, New York, 1966.

[31] A. Karim, A comparison between packed bed and wall coated reactors for the steam reforming of methanol, M.Sc. Thesis, Chemical Engineering Department, University of New Mexico, 2003.

[32] A. Karim, J. Bravo, K.A. Datye, Comparison of wall coated and packed bed reactors for the steam reforming of methanol, Chem. Eng. Sci., submitted for publication.